Stimulated Raman Scattering and its Applications in Optical Communications and Optical Sensors

O. Frazão[*,1,2], C. Correia[1], M.T.M. Rocco Giraldi[3], M.B. Marques[1,2], H.M. Salgado[1,4], M.A.G. Martinez[5], J.C.W.A. Costa[6], A.P. Barbero[7] and J.M. Baptista[1,8]

[1]*INESC Porto, Instituto de Engenharia de Sistemas e Computadores do Porto, Portugal*

[2]*Dept. de Física da Faculdade de Ciências da Universidade do Porto, Portugal*

[3]*Dept. de Engenharia Eléctrica, Instituto Militar de Engenharia, Brazil*

[4]*Dept. de Engenharia Electrotécnica e de Computadores da Faculdade de Engenharia da Universidade do Porto, Portugal*

[5]*Dept. de Engenharia Elétrica, Centro Federal de Educação Tecnológica Celso Suckow da Fonseca, Brazil*

[6]*Dept. de Engenharia Eletrônica, Universidade Federal do Pará, Brazil*

[7]*Dept. de Engenharia de Telecomunicações, Universidade Federal Fluminense, Brazil*

[8]*Dept. de Matemática e Engenharias, Universidade da Madeira, Portugal*

Abstract: This review presents the stimulated Raman scattering and its applications in three areas: optical amplification, multiwavelength lasers and optical sensing. It is presented the basic concept of the Raman Scattering (SRS) phenomenon focusing in the in-line distributed/discrete Raman amplification applications and in multiwavelength generation for optical communications. The use of stimulated Raman scattering in optical sensors is also reviewed. Finally, the recent use of photonic crystal fibers and waveguide devices to generate the Raman effect is also addressed.

INTRODUCTION

The nonlinear Raman phenomenon was observed by C. V. Raman in 1928. In 1971, the stimulated Raman scattering (SRS) in glass fiber was observed by Stolen *et al.* [1]. The same group in 1972 measured the Raman gain in single-mode fiber [2]. More recently, the SRS has been used for optical amplification in optical telecommunications in distributed or discrete signal amplification. Even if discovered many years ago [3] and highly investigated in the past [4], applications of Stimulated Raman Scattering (SRS) presented a renewed interest for compensation of optical losses in fibers transmissions [5], for the development of new tunable laser sources [6] or for low noise amplification of optically carried radiofrequency signals. For all these purposes, the optimization of devices is based on a compromise between three factors: the Raman nonlinearity of the optical medium, the interaction length and the pump beam intensity [4]. Research on Raman amplification in optical fibers started early in the 1970s [1]. The advantages from Raman amplification in the transmission fiber were studied since the mid-1980s [7, 8]. But, around 1995, when the maturity of suitable high power pump lasers was achieved [9] new interest in Raman amplification emerged. Researchers have showed some of the advantages that Raman amplifiers have over EDFAs, particularly when the transmission fiber itself is used as a Raman amplifier [10, 11]. This enabled to increase the advances in Raman amplifier technology [12]. Some of these advances are the novel Raman pumping schemes recently used in transmission experiments. The main newly schemes studied are: co-pumping for broad-band amplifiers, in which the OSNR tilt across the signal band is compensated [13, 14]; time-dependent Raman counter-pumping scheme where impairments such as pump-pump FWM [15] and the OSNR tilt [16] are seriously reduced [17-21] and high-order Raman pumping scheme to improve the span noise figure in a counter-pumping configuration or for a co-pumping scheme, allows more signal power to be launched before nonlinear distortions dominate [22, 23]. Recently, there has been much investigation in order to obtain devices to amplify or generate light using stimulated Raman scattering in silicon [24]. The Raman coefficient of silicon is several orders of magnitude larger than silica [25], thus reducing the needed interaction lengths for stimulated Raman scattering and optical gain to practical lengths for planar waveguides [26]. The modal area in a silicon waveguide is about 100 times smaller than in optical fiber, which results in a proportional increase in optical intensity. The consequence is that it enables to develop chip-scale Raman devices that in general need kilometers of fiber to work [27]. Planar waveguide Raman amplifiers and lasers have already been showed in the GaP material system [28]. As the first order Raman scattering shift in silicon is 15.6 THz and the 1400-1500 nm wavelength range high power pump lasers are already commercially available, Raman amplification is a pos-

*Address correspondence to this author at the INESC Porto, Instituto de Engenharia de Sistemas e Computadores do Porto, Portugal; Tel: (+351) 226012301; Fax: (+351) 226012799; E-mail: ofrazao@inescporto.pt

1874-3285/09

sibly implementable and attractive result for providing narrowband gain or lasing in silicon-on-insulator waveguide devices at the wavelengths for telecommunications [26]. The first experiment of spontaneous Raman emission in silicon waveguides in 2003 [24] was followed by the demonstration of stimulated Raman scattering [25] and parametric Raman wavelength conversion [29]. The Raman effect in silicon is advantageous since it does not need rare earth dopants and its spectrum is widely tunable through the pump laser wavelength. The use of germanium in the nonlinear Raman processes in silicon presents new possibilities for adjusting the device characteristics. Recently, the first GeSi optical Raman amplifier and laser were demonstrated [30]. The results indicate that the spectrum of Raman scattering can be tailored using the GeSi material system. Therefore, GeSi Raman devices represent a stimulating subject for future research and development.

In this work, the authors present an overview of stimulated Raman scattering and its applications in three distinct areas: Raman amplification for optical telecommunications, multi-wavelength lasers and distributed optical sensing. Recent advances in Raman using photonic crystal fibers and waveguide devices are also reported.

BASIC CONCEPT

Stimulated Raman scattering in optical fibers is an important nonlinear phenomena which arises from the interaction of an intense light beam (usually called pump) with the vibrational modes of the fiber silica molecules when such high pump power levels propagate throughout the fiber. During the scattering process, an optical phonon induces the molecule to make a transition to an excited vibrational state of energy $\hbar\omega_v$ and as a consequence the scattered photon of energy $\hbar\omega_s$ is red shifted with respect to the pump energy ($\hbar\omega_p$) by an amount equals to the difference between the pump energy and the excited vibrational state energy. The scattered light also called Stokes light frequency is $\omega_s = \omega_p - \omega_v$. An anti-Stokes light of frequency $\omega_{as} = \omega_p + \omega_v$ can also be scattered by the fiber silica molecule; nonetheless it requires an initially populated excited vibrational state. The anti-Stokes process is less efficient and consequently is not so important for silica fibers. Fig. (**1**) presents an optical communication system using Raman amplification. The signal propagates from the transmitter (Tx) to the receiver (Rx). When the pump is traveling in the same direction of the signal it is called "the co- or forward pump". If in the opposite direction it is called the "counter- or backward pump".

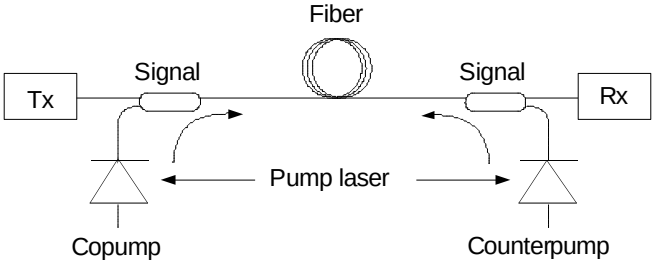

Fig. (1). Schematic of an optical communication system employing Raman amplification.

The Raman gain spectrum is the intensity of the Stokes light as a function of the Raman shift (frequency shift), $\Delta\omega$, i.e, the frequency difference between pump and the Stokes or signal light beam. The measured Raman gain efficiency spectra are shown in Fig. (**2**) for two different fibers: TrueWave® Reach Low Water Peak (LWP) and a Standard Single Mode Fiber (SMF). The maximum Raman gain efficiency occurs when the frequency difference is around 13.2 THz. The Raman gain is defined over a 40THz frequency range, and the gain peak is inversely proportional to effective core area [3].

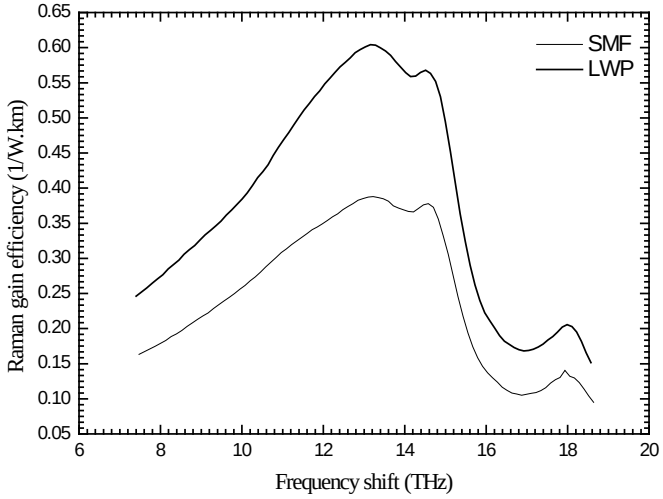

Fig. (2). Raman Gain Efficiency for the SMF and LWP fibers for a pump wavelength of 1453 nm.

For ultra-wide band Raman amplifiers a reliable estimative of the Raman gain spectrum for other pump wavelengths can be obtained using equation (1) [31]:

$$C_R^E(\lambda_P, \lambda_S) = \frac{\lambda_i}{\lambda_S}\frac{A_{eff}(\lambda_i)}{A_{eff}(\lambda_S)} C_R^M(\lambda_k, \lambda_i) \tag{1}$$

In Equation (1), $C_R^M(\lambda_k, \lambda_i)$ and $A_{eff}(\lambda_i)$ are the measured Raman gain efficiency and fiber effective core area at pump and signal wavelength λ_k and λ_i respectively, meanwhile $C_R^E(\lambda_P, \lambda_S)$ and $A_{eff}(\lambda_S)$ are the estimated Raman gain efficiency and fiber effective core area at the desired pump and signal wavelength λ_p and λ_s respectively.

The intensity of the stimulated scattered light grows exponentially once the incident pump power exceeds a certain threshold value. The threshold pump power P_{th} is defined as the incident power at which half of the pump power is transferred to the Stokes field at the output end of a fiber of length L [32]. The threshold pump power satisfies the condition [33]:

$$P_{th} \approx \frac{16}{L_{eff} C_R} \cong \frac{16\,\alpha}{C_R} \tag{2}$$

where L_{eff} is the fiber effective interaction length in meters and can be approximated by $1/\alpha$, since $\alpha L >> 1$, in practice; α represents fiber losses in m^{-1}.

$C_R = g_r / A_{eff}$ is the peak Raman gain efficiency value in 1/Wm, g_R is the peak Raman gain value in m/W and A_{eff} is the fiber effective core area in m^2.

In Table **1**, typical Raman gain coefficient, effective core area, Raman gain efficiency and attenuation are shown for the LWP and standard SMF fibers. The pump threshold values are calculated using Equation (2) for a pump wavelength at 1453 nm. The pump threshold power value for the standard SMF is around 69% above the LWP value. This is a consequence of the standard SMF larger effective area (68%).

The field propagation equation for optical beams propagating inside a bi-directional multi-channel WDM optical system distributed Raman amplifier, containing the main propagation phenomena, is represented by Equation (3) [34].

Equation (3) assumes that the pump and signal fields are in the form of CW beams. Even though the pump wave is usually continuous in optical fiber communications systems, the signal wave is generally in the form of a bit stream. However, the CW theory can still be applied to such systems since the signal power can be assumed as the average channel power. In fact, the Raman response is fast enough that the entire bit stream can be amplified without any distortion [43]. On the other hand, when very short pulses (less than 10 ps) are included, it is important to take into account the dispersive and nonlinear effects that are likely to affect the amplification of such short pulses in a Raman amplifier such as self-phase modulation (SPM), cross-phase modulation (XPM) and walk-off [43]. When both the pump and signal fields are in the form of a pulse train, due to the dispersive nature of silica fibers, the pump and signal pulses propagate with different group velocities because of their different wavelengths. Thus, although these pulses overlap initially, they separate after the walk-off distance. At the same time, the nonlinear effects such as SPM and XPM become important and influence considerably the propagation of the pump and signal pulses throughout the optical fiber [43]. Nevertheless, it is important to mention that generally Equation (3) is valid since the signal pulse is > 10 ps and the pump field is in the form of a CW beam, what usually occurs in lightwave systems.

The first three terms in the right hand side of Equation (3) represent linear effects while the remaining ones represent nonlinear effects. The description of each term follows:

- ***1st Term*** - Accounts for the attenuation or losses in the fiber due to material absorption, scattering due to defects in the waveguide, ultraviolet and infrared absorptions, among others.
- ***2nd Term*** - Accounts for the Rayleigh scattering, double Rayleigh scattering (DRS) and their multiple backscattering.
- ***3rd Term*** - Accounts for Stimulated Raman Scattering (SRS) from higher frequency to smaller frequency fields.
- ***4th Term*** - Accounts for the amplified spontaneous emission (ASE) generation and the influence of thermal noise.
- ***5th Term*** - Accounts for the depletion of the higher frequency fields due to vibrational losses.
- ***6th Term*** - Accounts for the loss due to amplified spontaneous emission influenced by thermal noise and losses due to vibratory movements. The factor of "2" is due to the uncorrelation between thermal noise and ASE signals.

$$\begin{aligned}\frac{\partial P_z^{\pm}(f_i)}{\partial z} = {} & \mp\alpha P_z^{\pm}(f_i) \pm \eta P_z^{\mp}(f_i) \pm P_z^{\pm}(f_i).\sum_{j=i}^{i-1}\frac{g_R(f_j-f_i)}{\Gamma A_{eff}}[P_z^{\pm}(f_j)+P_z^{\mp}(f_j)] + \\ & \pm hf_i.\sum_{j=i}^{i-1}\frac{g_R(f_j-f_i)}{\Gamma A_{eff}}[P_z^{\pm}(f_j)+P_z^{\mp}(f_j)].\left[1+\frac{1}{e^{[h(f_j-f_i)/KT]}-1}\right]\Delta\nu + \\ & \mp P_z^{\pm}(f_i).\sum_{j=i+1}^{n}\frac{f_i}{f_j}\frac{g_R(f_i-f_j)}{\Gamma A_{eff}}[P_z^{\pm}(f_j)+P_z^{\mp}(f_j)] + \\ & \mp 2hf_iP_z^{\pm}(f_i).\sum_{j=i+1}^{n}\frac{f_i}{f_j}\frac{g_R(f_j-f_i)}{\Gamma A_{eff}}[P_z^{\pm}(f_j)+P_z^{\mp}(f_j)].\left[1+\frac{1}{e^{[h(f_j-f_i)/KT]}-1}\right]\Delta\mu\end{aligned} \quad (3)$$

In Equation (3), α [1/m] is the attenuation coefficient or losses in fiber, η [1/m] is the Rayleigh scattering coefficient, g_R [m/W] is the Raman gain coefficient, Γ is the polarization factor of the fields in the waveguide ($\Gamma = 1$ if the optical fields present coherent polarization or $\Gamma = 2$ if the fields are depolarized [35]), A_{eff} [m^2] is the fiber effective core area, h [J/Hz] is the Planck constant, K [J/K] is the Boltzmann constant, f_i [Hz] is the spectral frequency and $\Delta\nu$ [m] and $\Delta\mu$ [m] are the noise bands. The vibrational losses are described by the reason between the frequencies of two fields (i and j) that are interacting between themselves (f_i / f_j).

In addition, the nonlinear terms are pair related, representing the power transfer among distinct terms, according to the principle of energy conservation. These power transfers will be made by Stokes waves, through the stimulated Raman scattering (SRS) effect, which will deplete the fields at higher frequencies and intensify the fields at smaller frequencies.

The propagation equation (Equation (3)) is modeled through a set of coupled [34, 36] stationary state equations [34], that scatter (SRS) a unidirectional wave, transferring power between co-propagating and counter-propagating fields. The equation becomes a contour problem, with two contour conditions located at the extremes of the optical fiber ($z = 0$ and $z = L$).

An algebraic solution of Equation (3) can be reached if we disregard the nonlinear terms. Although, the full propagation equation (Equation (3)) can be solved numerically using an approximate numerical method such as the Fourier's Split-Step method [37, 38], the Predictor-corrector method [34] or the Runge-Kutta method [39, 40].

Table 1. TrueWave® Reach - Low Water Peak and Standard Single Mode Fiber Parameters and Pump Threshold Power Values

	g_R [m/W]	A_{eff} [m^2]	C_R [1/Wm]	α [1/m]	α [dB/km]	P_{th} [W]
TrueWave® Reach LWP (λ_p = 1453nm)	3.42×10^{-14}	56×10^{-12}	0.61×10^{-3}	0.046×10^{-3}	0,20	1,21
Standard SMF (λ_p = 1453nm)	3.28×10^{-14}	82×10^{-12}	0.4×10^{-3}	0.044×10^{-3}	0,19	1,76

OPTICAL AMPLIFICATION

With the continued need for higher information capacity over increasingly longer transmission spans, optical amplifiers quickly became indispensable elements of optical communications networks. One of the enabling technologies [41] is Raman amplification, the main application of stimulated Raman scattering (SRS). Raman fiber amplifiers (RFAs) have low gains per unit length compared with erbium-doped fiber amplifiers (EDFAs) and semiconductor optical amplifiers (SOAs) [41]. Therefore long optical fiber spans are required to provide useful performance. The RFA guides light at both the signal and pump wavelengths and it is normally single mode to ensure the best overlap of all traveling waves. Highest gains are achieved by using fibers with small effective areas and low losses [42]. One of the great benefits of RFAs is that they do not require special dopants. The optical fiber can be one of the common types used for transmission or dispersion compensation. Moreover, as the spectral shape of the Raman gain depends primarily on the frequency separation between pump and signal (not their absolute frequencies) [8], gain can be provided at almost any wavelength by appropriate selection of the pump laser.

Because Raman gain does not depend on the relative direction of propagation of pump and signal [8], pumping can be co/forward, counter/backward or bidirectional with respect to the signal [43]. Co-directional pumping provides better performance from the noise viewpoint since the signal experiences amplification before decaying, but suffers from elevated nonlinear effects due to higher signal levels. That is why counter-directional pumping is often preferred. Backward launching also minimizes the transfer of relative intensity noise (*RIN*) from the pump laser to the signal. Moreover, it averages any polarization-dependent gain. Bidirectional pumping offers the best of both schemes at the cost of an extra pump. Another possibility is higher order pumping [44] to further reduce the noise figure (*NF*) of the amplifier by distributing the gain more evenly across the length of the fiber. Besides *RIN*-transfer and polarization dependent gain, RFAs have to deal with additional challenges including noise originating from (amplified) spontaneous Raman scattering and multipath interference caused by double Rayleigh backscattering. The flexibility of Raman amplification allows shaping the gain spectrum by combining multiple pump wavelengths [43]. Using this broadband pumping approach, amplifiers with gain bandwidths greater than 100 nm have been demonstrated [45]. They are particularly useful for amplifying (dense) wavelength division multiplexed (WDM) systems. However, these broadband RFAs suffer from strong Raman pump-pump interactions [46]. The short wavelength pumps amplify the longer wavelength pumps, and so more power is typically needed at the shortest wavelengths. This interaction between the pumps also affects the noise properties of broadband amplifiers and results in noise figure tilt. Broadly speaking, there are two classes of Raman amplifiers [42]. One class is distributed Raman amplifiers, so called because the gain is distributed along the fiber span. Another class is called discrete/lumped Raman amplifiers because the signal gain occurs within discrete elements in the transmission system. Naturally, the two classes can be combined to form a hybrid amplifier, where the discrete RFA can be replaced by an EDFA [47]. The term distributed amplification refers to the method of cancellation of the intrinsic fiber loss. In an ideal distributed amplifier, the loss is counterbalanced at every point along the span. The transmission fiber is in fact turned into an amplifier. As a consequence the SNR is improved when compared to (ideal) discrete amplification. This improved noise performance may be used in different ways. One way is to extend the reach between repeaters, another is to extend the total reach of a transmission system, and finally a third is to improve the transmission capacity. An elaborate investigation that demonstrated the application of distributed Raman amplification as a means to upgrade existing systems was reported in 1997 [48]. A power budget improvement of 7.5 dB was demonstrated by launching 1.0 W of 1423 nm pump light from the receiver end. This improvement was sufficient either to increase the bit-rate in a single channel from 2.5 Gb/s to 10 Gb/s or to increase the channel count from one 10 Gb/s to four 10 Gb/s channels centered around 1550 nm. In the following years multiple experiments showed continued improvements in reach between repeaters, total span length and transmission capacity [49]. Single channel bitrates evolved from 10 Gb/s to 160 Gb/s [50] and even a record-breaking 320 Gb/s [51]. In multi-channel communication the most common bit rate for a single-channel nowadays remains at 40 Gb/s. In 2001, researchers were able to combine up to 270 channels to create a massive WDM system which is capable of handling bitrates up to 10 Tb/s over 117 km [52]. This is accomplished by using the S-, C- and L-bands. Other experiments include also the U-band [53]. Recently a 25.6 Tb/s experiment was demonstrated over a 240 km repeatered span by employing 160 WDM channels with 50 GHz channel spacing in the C- and L-bands (see experimental configuration in Fig. (**3**)) [54]. Each channel contained two polarization-multiplexed 85.4 Gb/s RZ-DQPSK signals, yielding an impressive spectral efficiency of 3.2 b/s/Hz in each band. Simultaneously with growing transmission capacity, increasingly larger reach between repeaters and total span length are realized.

In one experiment second-order backward pumping and forward pumping were combined to establish 500 km long unrepeatered transmission of 16 × 10 Gb/s RZ-DPSK signals [55]. Another experiment demonstrates trans-pacific (10000 km) 40 Gb/s transmission using all Raman amplified 100 km spans, SRZ-DPSK and enhanced forward error correction [56].

Other experiments include the applicability of special fibers like silica core PCF [57]. Incoherent pump sources also become interesting to further improve the RFA technology. More specifically they improve the gain flatness (while using less pump lasers when compared to coherent pumping) and the polarization insensitiveness at the cost of a small degradation of the noise figure at the shorter wavelengths [58-59]. However, more research is necessary.

Researchers also experiment with alternative configurations of RFAs. In one experiment optical phase conjugation is performed in the middle of the span to compensate for the nonlinear signal distortions and to diminish signal fluctuation. In this manner a 46 nm broadband WDM system was realized while simultaneously limiting the power fluctuation of the signals to 3.5% and the gain ripple to 5.3 % [60]. Simultaneously, a number of authors [61-63] abandon the big-

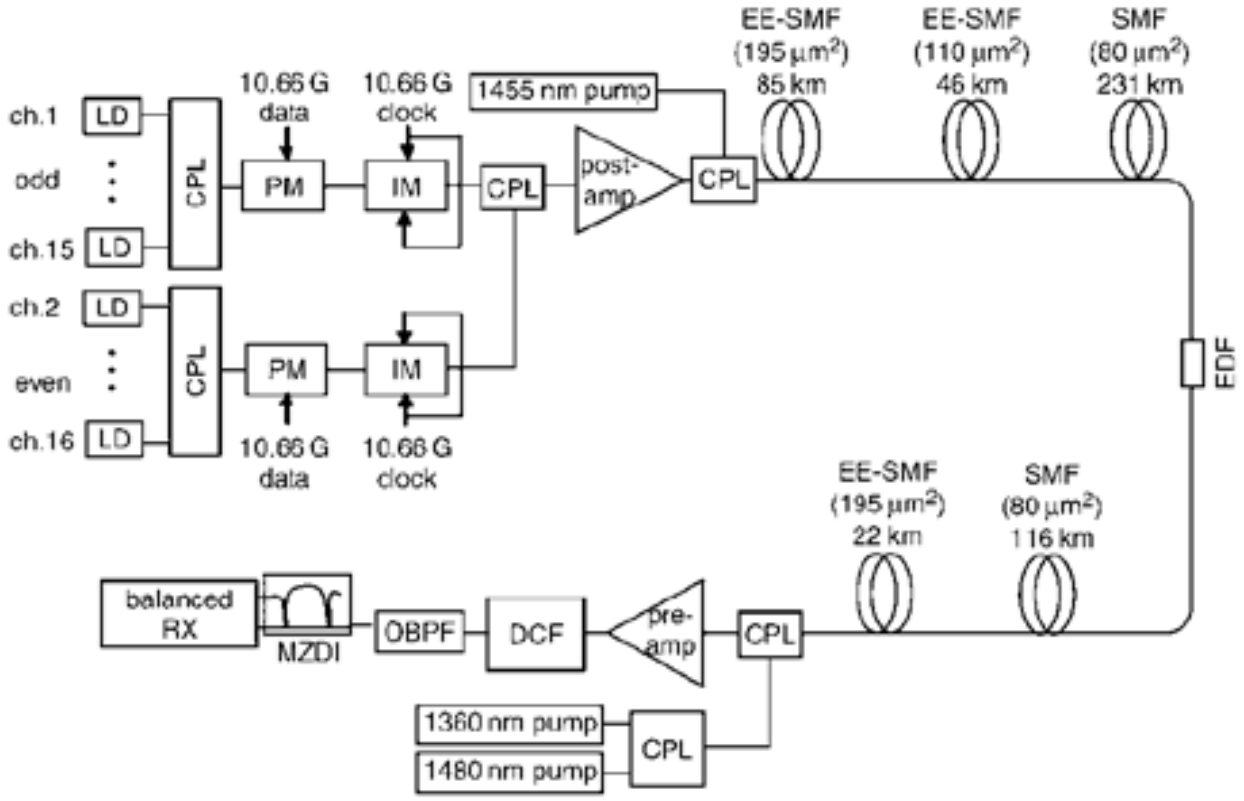

Fig. (3). Experimental setup at 160 WDM channels with 50 GHz channel spacing in the C- and L-bands [54].

ger and better philosophy and focus on larger operating margins to produce systems ready for industry deployment.

This class of RFAs is called discrete because they provide amplification at specific points along the transmission span. The fiber lengths used are a lot shorter (order tens instead of hundreds of km) when compared to distributed RFAs. And because gain accumulates with fiber length, Raman amplification better fits in the latter amplifier class. Though, discrete Raman amplifiers have many attractive aspects over rare-earth-doped fiber amplifiers such as EDFAs including arbitrary gain band, better adjustability of gain shape and better linearity [41].

On the other hand, the pump-to-signal power conversion efficiency (PCE) of a discrete RFA is very low as compared with EDFAs, which can easily achieve several tens percent of power conversion efficiency [64]. However, the PCE of a Raman amplifier can be increased by using higher input power, because the gain of a Raman amplifier has a larger saturation power than an EDFA. In one experiment an average power conversion efficiency of 27% is achieved for a total input signal power of 0.04 dBm [65]. Another important performance measure is the noise figure. Discrete Raman amplifiers with noise figures as low as 4.2 dB have been reported [66]. In this paper, such a low NF was achieved by means of (*i*) a short length and high efficiency of the gain fiber, (*ii*) a two-stage amplifier configuration with an intermediate isolator to block the Rayleigh backscattered signal, and (*iii*) a high pump power. Besides its obvious use, discrete Raman amplification is very often employed in dispersion-compensating modules to overcome their loss or even provide some gain to also address the losses of constituent components such as filters, isolators and connectors [67, 68]. In spite of the short fiber lengths, the dispersion-compensating fiber (DCF) used in these modules provides enough gain thanks to its small effective core area and high doping level of Germanium [69]. In one example of a dispersion-compensating Raman amplifier it is possible to completely compensate for the losses and to lower the NF by at most 1.5 dB [70]. Other examples include C+L-band dispersion-compensating Raman amplifier for SMF transmission links [71], S-band dispersion -compensating Raman amplifier for SMF [70] and 100-nm bandwidth dispersion-compensating Raman amplifier for SMF [71].

MULTIWAVELENGTH LASER

Raman scattering can be also used for other applications, usually in configurations that implement multiwavelength Raman fiber lasers. In the last years, this type of configuration deserved lots of attention, mainly for applications that require high transmission capacity demand in optical communications (i.e., wavelength division multiplexing (WDM) and dense wavelength division multiplexing (DWDM)) [72].

Multiwavelength generation based on Erbium doped fibers (EDF) has been extensively reported in the past [73]. This specific generation method shows some disadvantages; namely: the suppression of the homogenous line broadening and an unstable gain competition for a stable multiwavelength operation at room temperature. Raman fiber laser implementation in multiwavelength generation appears as a potential and prosperous solution to avoid the aforesaid dis-

advantages. Multiwavelength generation based on Raman shows also the advantage of an extremely large bandwidth (only limited by the numbers of pumps wavelength available for improved gain flatness). These characteristics are extremely helpful in WDM generation.

Multiwavelength Raman lasers have been studied and developed in different configuration types, incorporating fiber Bragg gratings [74], long-period fiber gratings [75], Sagnac loop mirrors [76], Fabry-Perot filters, etc. The main characteristic of multiwavelength fiber lasers is their channel spacing, which should be tunable in order to provide a flexible and a functional design. In the next paragraphs the fundamental works carried out in this area will be discussed.

Matos *et al.* [77] developed one of the first works in the area, in a fiber Bragg grating (FBG) Raman ring fiber laser configuration. Four lasing wavelengths were obtained with a channel spacing of ~5 nm. The four channels show a line width of approximately 0.6 nm and signal-noise ratio (SNR) higher than 40dB. The main advantage of this configuration is that an increase in the FBG counts enlarges the channel number and consequently improves its tunability.

On the other hand, using a Fabry-Pérot filter in the cavity of a Raman fiber ring laser was possible to generate over 58 WDM channels with 50GHz channel spacing. The WDM multiwavelength shows a stable operation for the entire channels with an extinction ratio of ~50 dB. Modifying the pump wavelengths and the pump power ratio several operation ranges could be obtained [78].

In 2003, Kim *et al.* [79] presented a cascaded Raman fiber ring laser using a tunable dual section high birefringence fiber Sagnac loop filter. In this configuration, the position of a single (or multiple) Stokes wave is controlled by the pump power and the cavity. Tuning the above parameters the source operates between 1.12 nm and 1.58 nm. The authors generated more than 20 lasing wavelength with a channel spacing of 0.4 nm.

At the same time, Han *et al.* [75], proposed a multiple wavelength generation with the introduction of a cascaded of long period gratings (LPGs) as multichannel fiber filter (Fig. **4**). Since the LPG is a simple and flexible multichannel filter, it is an effective method to generate multiple wavelengths. Based on this method it is obtained up to five WDM channels with SNR higher than 20 dB in the L-band. Depending on physical parameters of cascaded LPGs (i.e., grating distances, grating length and number of gratings) several results can be achieved. One year later, the characteristics of a tunable multiwavelength semiconductor and a tunable multiwavelength all-fiber-built Raman fiber laser were compared by Chen *et al.* [80].

To get a tunable wavelength spacing a high birefringence fiber loop mirror (HiBi-FLM) is used [76].

The number of lasing wavelengths was determined by the total insertion loss of the HiBi-FLM, as well as the gain bandwidth of the amplifier. It was obtained four or five lasing wavelengths with a spacing of 3.2 nm and 1.6 nm, respectively. Both lasers exhibited stable operation at room temperature and selectable wavelength spacing.

Han *et al.* [72], developed different configurations of the tunable multi-wavelength Raman laser setup (Fig. **5**). They found that modifying some of the components, the number of channels could experiment some variation. The first work was based on a FBG cavity with polarization maintaining fiber (PMF) Lyot-Sagnac filter. The number of channels and wavelength spacing of the multi-wavelength fiber laser were controlled by the two PMF segments in the intra-cavity of the filter. Based on this configuration, seven channels with 0.6 nm-spacing wavelengths and five channels with 0.8 nm-spacing wavelengths were achieved at room temperature.

In further articles, Han *et al.* substituted the Lyot-Sagnac filter by a tunable chirped FBG with high reflectivity and a phase-shifted FBG [81]. The authors also used similar Fig. (**5**) configuration and a modified sensing head formed by two uniform FBGs with different cladding diameter [82]. In the above two methods two channel generation with an extinction ratio of more than ~50dB were obtained.

Han *et al.* [83] also proposed a tunable multiwavelength Raman fiber laser based on Bragg grating written in a few-mode fiber and follow the similar configuration shown in Fig. (**5**). In this system, the number of lasing wavelengths can be adjusted by the properties of few-mode Bragg grating. Thus, the lasing wavelength of the multiwavelength Raman fiber laser could be effectively controlled depending on the direction of the bending curvature of the FBG when it is glued in a flexible metal plate. Based on this method, it is

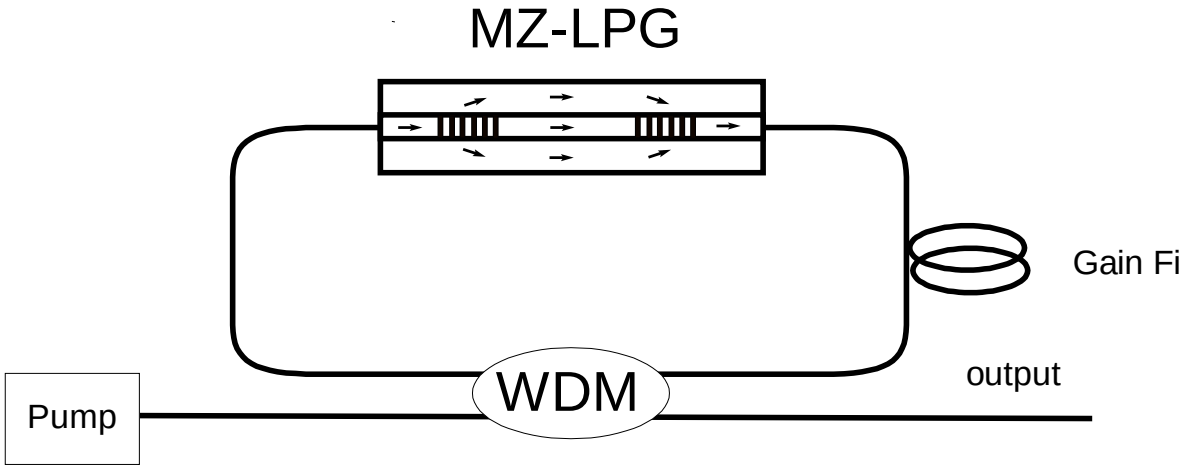

Fig. (4). Multiwavelength Raman laser using MZ-LPG [72].

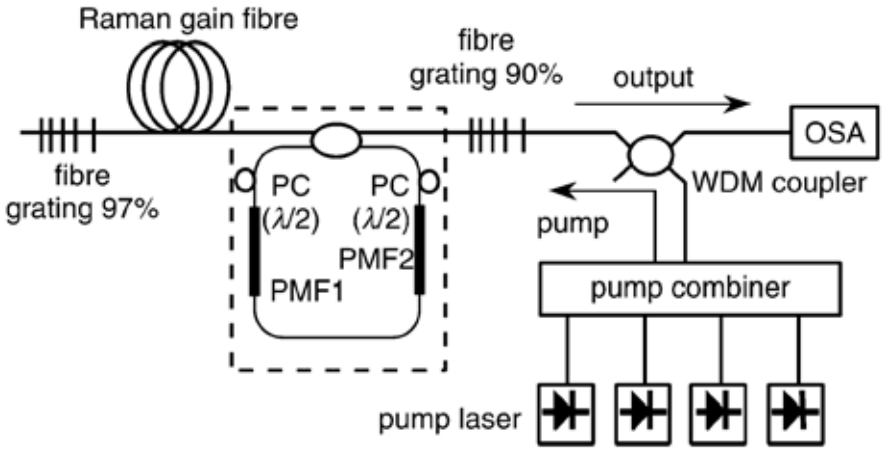

Fig. (5). Experimental setup for tunable multi-wavelength Raman laser based on FBG cavity incorporating PMF Lyot Sagnac filter [72].

achieved high quality Raman laser output with SNR higher than 45 dB and a bandwidth less than 0.12 nm in each channel. The wavelengths of the laser can be changed with FBG curvature in a dynamic range of more than 15 nm.

Replacing the few-mode Bragg grating of the above work by multiples few-mode Bragg gratings, Han *et al.* [84] obtained three-channel Raman laser output with an extinction ratio of more than 45 dB. This result is similar as the last reported; but with the improvement that is not necessary to implement curvature to the FBG. In this case, the lasing wavelengths are tuned by properly choosing the characteristics of the FBG.

In the same year, Wang *et al.* [85] proposed a multiwavelength generation employing sampled Bragg grating (SBG) in a Raman fiber ring configuration. The characteristics of the multiwavelength laser can be tuned adjusting the parameters of the SBG, such as: sampling period and sampling length. Using this method four oscillating wavelengths as well as five wavelength channels were achieved.

A novel free-spectral-range (FSR)-tunable comb filter based on a superimposed chirped-fiber Bragg grating (CFBG) and a linear cavity formed by a bandwidth-tunable CFBG reflector was also proposed. Dong *et al.* [76] presented a multiwavelength Raman fiber laser with an independently-adjustable channel number. The channel numbers were determined by the bandwidth of the CFBG reflector and the channel spacing. Multiwavelength laser operation with spacing tuning from 0.3 to 0.6 nm and channel number adjustment from 2 to 10 were achieved.

Recently, Ning *et al.* [86] implemented a multi-wavelength Raman fiber laser inserting a sampled chirped FBG. Adjusting the polarization controller in the ring cavity up to ten stable wavelengths with equalized peak power and SNR of ~50dB are achieved at room temperature.

Generation systems based on multiwavelength Raman fiber are quite useful in several applications (i.e., in optical communication systems with high transmission capacity and in long-distance remote sensing systems). Multiwavelength fiber lasers have also the advantages of simple structure, equalized peak power and simple fabrication with low cost. In the next section, several results employing Raman multiwavelength generation as a remote sensor are presented.

OPTICAL SENSING

Previously, it was analyzed all the characteristics of Raman effect for amplification and multiwavelength generation (i.e., bandwidth, gain, spectral response, noise figure, output power, etc). Moreover, Raman scattering can be easily used in other applications that do not include amplification. Raman effect has also been studied over the years as an optical fiber distributed temperature sensor [87-89]. It was particularly attractive, because the system only needed a single pump source in all the sensing structure, reducing the network's cost and complexity [90]. Different configurations have been developed in order to measure changes in temperature, incorporating EDF, FBG, chirped FBG, etc. Its purpose was to obtain higher precision and sensitivity and larger output range along the kilometers of conventional silica fiber. In the early 90s, most commercial Raman sensors for distributed temperature were based on Raman optical time reflectometry (ROTDR). In this configuration a short pulse is sent along the fiber and the backscattered Raman light is detected. In 1999 it was reported a method to use the spontaneous Raman scattering for remote sensing, where the ROTDR method was applied. To accomplish the remote sensing, Farahani *et al.* [88] analyzed the behavior of different types of fibers. They achieved that the best results were obtained when a probe wavelength of 1550 nm is employed in a single-mode fiber over a maximum distance of 10 km.

In the same year, Kee *et al.*, developed a Raman-based distributed temperature sensing (DTS) system for temperature monitoring [87]. This work achieved a distance greater than 10 km in single-mode silica fiber, with a temperature resolution of 4ºC. Grating based devices (i.e. FBG, SBG, phased-shifted FBG, chirped FBG, LPG, etc) are truly helpful for distributed sensing application. Using FBGs simultaneously with a proper power source (like a Raman laser) an advantage of higher resolution in wavelength shift and higher optical SNR is obtained [91]. Peng *et al.* [92], proposed a linear cavity fiber laser configuration based on a fiber Bragg grating sensor. The medium gain is done by the distributed Raman amplifier. In this configuration since two FBG are used, when the wavelength of FBG2 drifted no influence on the lasing wavelength of FBG1 is exhibited. In this case, the strain sensitivity was 2.27 nm/με for a sensing distance near to 25 km. The use of multiple laser cavities

based on FBGs and a tunable chirped FBG was proposed by Lee. The temperature sensitivity in this configuration shows a linear response of 7.15 pm/ºC. The Raman lasers have a high stability and an extinction ratio greater than 50 dB over the 50 km [93]. Afterwards, the authors improved the configuration of the system in order to obtain simultaneously strain and temperature sensitivity [94].

Full details of the principle of cascading, a sensing probe of an erbium-doped fiber (EDF) and a FBG, for simultaneous measurement of temperature and strain can be found in [95] (Fig. **6**). The sensing distance was also higher than 50 km with a temperature sensitivity of 8.19 pm/ºC in a range from 30 ºC to 100 ºC.

On the other hand, a strain sensitivity of 1.1 pm/με was observed. In 2005, Han *et al.* [86] upgraded their system, adding multiple phased-shifted FBGs and a tunable high reflection chirped FBG. In this case, the temperature and strain sensitivities were found to be 10.1 pm/ºC and 7.5 pm/με, respectively. In June of the same year, the same group obtained an output with two channels.

The two generated peaks showed the equivalent temperature sensitivity but different strain sensitivity. A temperature sensitivity in each channel was measured to be 9.5 pm/ºC with a minimum 5.3 pm/με for strain sensitivity. These results were obtained by the improvement of the configuration, due to the addition of two uniform FBGs with different cladding diameters [82]. Cho *et al.*, studied a distributed Raman amplification combined with a remotely pumped Erbium doped fiber amplifier (EDFA) in order to enhance the performance of spontaneous Brillion-based distributed temperature sensors. Based on this configuration a temperature resolution of 5.7ºC with a spatial resolution of 20 m in a distance of 88 km was achieved [96]. Sensor availability range is an important parameter and a lot of efforts have been carried out in order to increase this parameter. Usually, these efforts include the increasing of the pump power, which is limited by the cost and the nonlinear problems. The abovementioned increase results also in a degradation of the sensor performance. Gong *et al.* [97] proposed a new method based on ROTDR to enlarge the sensing distance. They found a theoretical solution using different type of fibers, which increases the Raman gain efficiency (g_R/A_{eff}). This is a good alternative in the near future; however it is not easy to perform due to the lack of fibers with different g_R/A_{eff}. Recently, Chakrasborty [98] exposed a novel form to compensate the temperature dependence in the Stokes signal and projected a method to carry out a dynamic self-calibration of the Raman distributed temperature sensor. The temperature dependence of the Stokes signal introduced several errors and proved that this effect degrades the signal over the 90%. The abovementioned discussion shows that distributed Raman fiber-optic sensors provide an excellent method to measure temperature over long distances, which is normally limited up to 25 km due to Rayleigh scattering. In the near future, it is expected that Brillion and Raman scattering will be investigated simultaneously in order to reach better results.

PHOTONIC CRYSTAL FIBER TECHNOLOGY

Photonic crystal fiber (PCF) represents a promising opportunity for the development of devices based on Raman effect. On advantage of this technology is to reduce the fiber length and the power levels required. Yusoff *et al.* [99] presented the first preliminary results in photonic crystal fiber for Raman amplification and for an all optical Raman Modulator. Fuochi *et al.* [100] reported an analysis of the Raman properties in triangular photonic crystal fiber. Here, it was also investigated how the presence of the germanium doped core can influence the Raman properties. Bottaccini *et al.* [101] have developed a model of photonic crystal fiber amplifiers. The PCF with germanium doped can enhance the gain for the same pump power. Finally, stimulated Raman scattering in ethanol core PCF was demonstrated by Yiou *et al.* [102]. This new approach of PCF with ethanol or with another liquid opens new development perspectives for stimulated Raman scattering nonlinear properties with applications in optical communications and sensing.

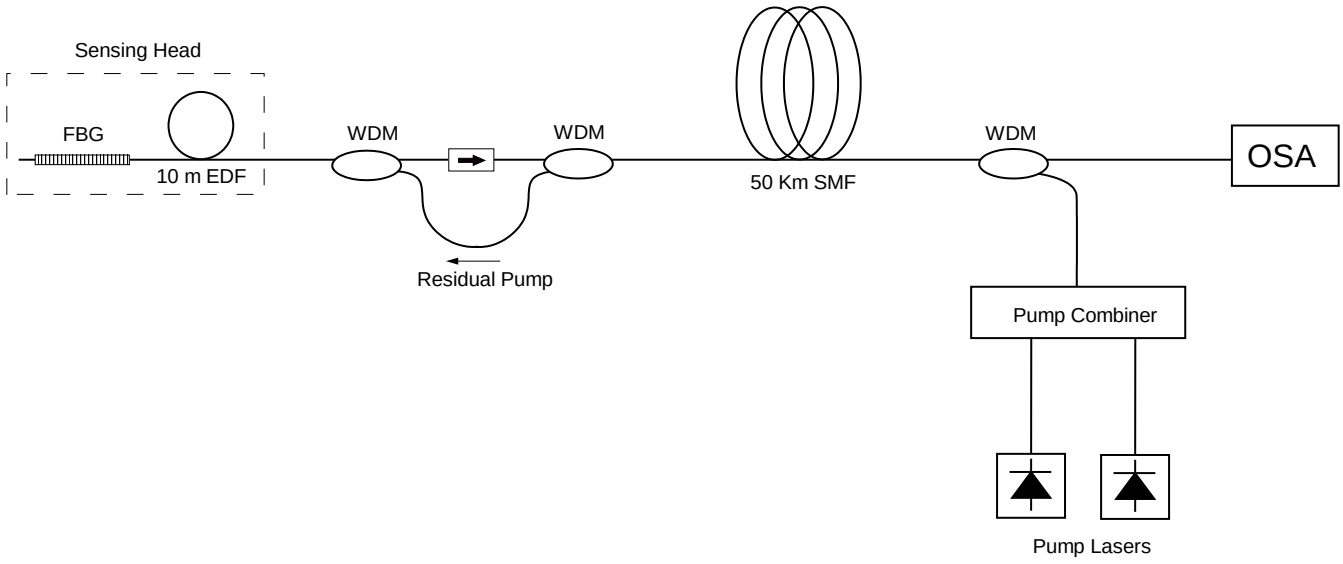

Fig. (6). Simultaneous measurement of strain and temperature combined two different technologies [95].

WAVEGUIDE TECHNOLOGY

In the last years, several investigations about Raman effect were accomplished in others technologies besides silica fiber. The goal was to discover and obtain new possibilities for laser generation and optical amplification using the SRS in waveguide technology. The waveguide can be performed in several materials but is widely fabricated in silicon [103]. The use of silicon waveguides is based on Raman gain coefficient, in other words, is used because the silicon presents a gain coefficient that is several times larger than that of standard glass. This is a seducing characteristic for amplification since it is possible to obtain high gains in small lengths. As it was reported by Claps *et al*., [104] this gain can be up to 10 db in only a 2cm silicon waveguide. Using this same SRS principle it is possible to provide a mean to generate optical gain in a silicon waveguide in order to obtain high power Raman lasers [105]. Obviously, the silicon waveguiding technology presents some disadvantages when compared with optical fiber technology; one of them is caused by losses on coupling light from the fiber to the waveguide. However, the main drawback is the loss generated inside the waveguide, which limits the system performance. This last constraint is due to a nonlinear absorption called two-photon absorption (TPA) [106]. One can think that one way to counterbalance these losses is by increasing the pump power of the source, but in reality it is the key to increase the loss due to TPA. Generally, this free carrier generation is reported as an answer to explain the short amount of gain that is introduced in the system [26, 29]. In literature some solutions have been reported in order to improve the coupling efficiency and diminish the damaged of the TPA on waveguiding, but until now injecting the pump power in a surrounding cladding is the most successful one [107, 108]. The use of silicon waveguide has diverse application fields and with Stimulated Raman Scattering the performance of the integrated optical circuits can be improved, however it requires further investigation and analysis to overcome and understand all the difficulties of the use of silica as waveguides.

CONCLUSION

In summary, a review of stimulated Raman scattering and its applications was addressed. The basic concept of the Raman scattering phenomenon focusing in the in-line distributed/discrete Raman amplification applications and in multiwavelength generation for optical communications was presented. The use of stimulated Raman scattering in optical sensors was also addressed. Finally, recent advances in stimulated Raman scattering in photonic crystal fibers were also reported. The study of the Raman effect in new types of fibers, having different doping or geometry, has renewed the interest of the Raman effect for applications in optical communications and sensing.

REFERENCES

[1] Stolen RH, Ippen EP, Tynes AR. Raman oscillation in glass optical waveguides. Appl Phys Lett 1972; 20(2): 62-4.

[2] Stolen RH, Ippen EP. Raman gain in glass optical waveguides. Appl Phys Lett 1973; 22(6): 276-8.

[3] Stolen RH, Lee C, Jain RK. Development of the stimulated Raman spectrum in single mode silica fibers. J Opt Soc Am B: Opt Phys 1984; 1(4): 652-7.

[4] Eckhardt G, Hellwarth RW, McClung FJ, Schwarz SE, Weiner D, Woodbury EJ. Stimulated Raman scattering from organic liquids. Phys Rev Lett 1962; 9(11): 455.

[5] Desurvire E. Erbium-doped fiber amplifiers: principles and applications. New York: John Wiley & Sons; 1994.

[6] Frey R, Pradere F. Powerful Tunable Infrared Generation by Stimulated Raman-Scattering. Opt Commun 1974; 12(1): 98-101.

[7] Mollenauer LF, Gordon JP, Islam MN. Soliton Propagation in Long Fibers with Periodically Compensated Loss. IEEE J Quantum Electron 1986; 22(1): 157-73.

[8] Bromage J. Raman amplification for fiber communications systems. J. Lightwave Technol 2004; 22(1): 79-93.

[9] Grubb SG, Strasser T, Cheung WY, *et al.* High power, 1.48 μm cascaded Raman laser in germanosilicate fibers. Proc Optical Amplifiers and Their Application; 1995.

[10] Hansen PB, Eskildsen L, Grubb SG, *et al.* Capacity upgrades of transmission systems by Raman amplification. IEEE Photonics Technol Lett 1997; 9(2): 262-4.

[11] Nielsen TN, Stentz AJ, Hansen PB, *et al.* 1.6 T b/s (40 × 40 Gb/s) transmission over 4 × 100 km of nonzero-dispersion fiber using hybrid Raman/erbium-doped inline amplifiers. In: Proc. Europ. Conf. Optical Communications 1999.

[12] Tsukiji N, Yoshida J, Kimura T, Koyanagi S, Fukushima T. Recent progress of high power 14XX nm pump lasers. In: Active and Passive Optical Components for WDM Communication conference; Denver, USA 2001; pp. 349-360.

[13] Kado S, Emori Y, Namiki S, Tsukiji N, Yoshida J, Kimura T. Broadband flat-noise Raman amplifier using low-noise bidirectionally pumping source. In: Proc Europ Conf Optical Communications 2001.

[14] Zhu B, Leng L, Nelson LE, *et al.* 3.2 Tb/s (80 x 42.7 Gb/s) transmission over 20 x 100 km of nonzero dispersion fiber with simultaneous C + L-band dispersion compensation. In: Proc Optical Fiber Communications Conf; 2002.

[15] Neuhauser RE, Krummrich PM, Bock H, Glingener C. Impact of nonlinear pump interactions on broadband distributed Raman amplification. In: Proc Optical Fiber Communications Conf 2001.

[16] Fludger CRS, Handerek V, Mears RJ. Fundamental noise limits in broadband Raman amplifiers. In: Proc Optical Fiber Communications Conf; 2001.

[17] Fludger CRS, Handerek V, Jolley N, Mears RJ. Novel ultrabroadband high performance distributed Raman amplifier employing pump modulation. In: Proc Optical Fiber Communications Conf 2002.

[18] Winzer PJ, Sherman K, Zirngibl M. Experimental demonstration of time division multiplexed Raman pumping. In: Proc Optical Fiber Communications Conf 2002.

[19] Mollenauer LF, Grant AR, Mamyshev PV. Time-division multiplexing of pump wavelengths to achieve ultrabroadband, flat, backward-pumped Raman gain. Opt Lett 2002; 27(8): 592-4.

[20] Nicholson JW, Fini J, Bouteiller JC, Bromage J, Brar K. A swept-wavelength Raman pump with 69 MHz repetition rate. In: Proc Optical Fiber Communications Conf; 2003.

[21] Grant AR. Calculating the Raman pump distribution to achieve minimum gain ripple. IEEE J Quantum Electron 2002; 38(11): 1503-9.

[22] Rottwitt K, Stentz AJ, Nielsen TN, Hansen PB, Feder K, Walker K. 80-km bi-directionally pumped distributed Raman amplifier using second-order pumping. In: Proc Europ Conf Optical Communications 1999.

[23] Labrunie L, Boubal F, Brandon E, *et al.* 1.6 Terabits/s (160 x 10.66 G bit/s) unrepeatered transmission over 321 km using second-order pumping distributed Raman amplification. In: Proc Optical Amplifiers and Their Applications; 2001.

[24] Claps R, Dimitropoulos D, Raghunathan V, Han Y, Jalali B. Observation of stimulated Raman amplification in silicon waveguides. Opt Express 2003; 11(15): 1731-9.

[25] Ralston JM, Chang RK. Spontaneous-Raman-Scattering Efficiency and Stimulated Scattering in Silicon. Phys Rev B 1970; 2(6): 1858.

[26] Liang TK, Tsang HK. Role of free carriers from two-photon absorption in Raman amplification in silicon-on-insulator waveguides. Appl Phys Lett 2004; 84(15): 2745-7.

[27] Jalali B, Raghunathan V, Dimitropoulos D, Boyraz O. Raman-based silicon photonics. IEEE J Sel Top Quantum Electron 2006 May-Jun; 12(3): 412-21.

[28] Suto K, Kimura T, Nishizawa J. Fabrication and characteristics of tapered waveguide semiconductor Raman lasers. IEEE Proc Optoelectron 1996; 143(2): 113-8.

[29] Claps R, Raghunathan V, Dimitropoulos D, Jalali B. Anti-Stokes Raman conversion in silicon waveguides. Opt Express 2003; 11(22): 2862-72.

[30] Claps R, Raghunathan V, Boyraz O, Koonath P, Dimitropoulos D, Jalali B. Raman amplification and lasing in SiGe waveguides. Opt Express 2005; 13(7): 2459-66.

[31] Fiuza J, Mizutani F, Martinez MAG, Pontes MJ, Giraldi MTMR. Analysis of Distributed Raman Amplification in the S-Band over a 100 km. J of Microwaves and Optoelectronics 2007; 6(1): 323-34.

[32] Agrawal GP. Fiber-optic communication systems. 3rd ed. New York: Wiley-Interscience; 2002.

[33] Smith RG. Optical Power Handling Capacity of Low Loss Optical Fibers as Determined by Stimulated Raman and Brillouin Scattering. Appl Opt 1972; 11: 2489-94.

[34] Liu X, Lee B. A fast and stable method for Raman amplifier propagation equations. Opt Express 2003; 11(18): 2163-76.

[35] Kang Y. Calculations and measurements of Raman gain coefficients of different fiber types [M.S. thesis]. Virginia Polytechnic Institute and State University; 2002.

[36] Lopez-Barbero AP, Pontes MJ, Giraldi MTMR, *et al*. Numerical routines for the optimization of pumps power and wavelength in distributed Raman amplifiers. Fiber Integr Opt 2006; 25: 347-61.

[37] Hodžić A. Investigations of high bit rate optical transmission systems employing a channel data rate of 40 Gb/s [Ph.D. Thesis]. Fakultät Elektrotechnik und Informatik der Technischen Universität Berlin; 2004.

[38] Iannone E. Nonlinear optical communication networks. New York: Wiley & Sons; 1998.

[39] Zill DG. A first course in differential equations with applications. 4th ed. Boston: PWS-Kent; 1989.

[40] Edwards CH, Penney DE. Elementary Differential Equations, 5th ed. Prentice-Hall; 2003.

[41] Urquhart P, Lopez OG, Boyen G, Bruckmann A. Optical Amplifiers for Telecommunications. In: IEEE International Symposium on Intelligent Signal Processing 2007; pp. 1-6.

[42] Mandelbaum I, Bolshtyansky M. Raman amplifier model in single-mode optical fiber. IEEE Photon Technol Lett 2003; 15(12): 1704-6.

[43] Headley C, Agrawal GP. Theory of Raman Amplifiers. Chap. 2. In: Raman Amplification in Fiber Optical Communication Systems. Elsevier, academic Press 2004; 33-97.

[44] Faralli S, Bolognini G, Sacchi G, Sugliani S, Di Pasquale F. Bidirectional higher order cascaded Raman amplification benefits for 10-Gb/s WDM unrepeated transmission systems. J Lightwave Technol 2005; 23(8): 2427-33.

[45] Emori Y, Tanaka K, Namiki S. 100 nm bandwidth flat-gain Raman amplifiers pumped and gain-equalised by 12-wavelength- channel WDM laser diode unit. Electron Lett 1999; 35: 1355-6.

[46] Kidorf H, Rottwitt K, Nissov M, Ma M, Rabarijaona E. Pump interactions in a 100-nm bandwidth Raman amplifier. IEEE Photonics Technol Lett 1999; 11(5): 530-2.

[47] Carena A, Curri V, Poggiolini P. On the optimization of hybrid Raman/erbium-doped fiber amplifiers. IEEE Photon Technol Lett 2001; 13: 1170-2.

[48] Hansen PB, Eskildsen L, Grubb SG, *et al.* Capacity upgrades of transmission systems by Raman amplification. IEEE Photonics Technol Lett 1997; 9(2): 262-4

[49] Evans A. Raman amplification in broadband WDM systems. In: Optical Fiber Communication Conference; 2001. pp. TuF4-1-TuF4-3.

[50] Weisser S, Raddatz L, Benz A, *et al.* Singlechannel 170 Gbit/s transmission up to 4000 km using dispersion-managed fiber spans and all-4 Raman amplification. In: European Conference on Optical Communication 2005; pp. 439-40.

[51] Mikkelsen B, Raybon G, Essiambre RJ, *et al.* 320-Gb/s single-channel pseudolinear transmission over 200 km of nonzero-dispersion fiber. IEEE Photonics Technol Lett 2000 Oct; 12(10): 1400-2.

[52] Fukuchi K, Kasamatsu T, Morie M, *et al.* 10.92-Tb/s (273/spl times/40-Gb/s) triple-band /ultra-dense WDM optical-repeatered transmission experiment. In: Optical Fiber Communication Conference 2001. pp PD24 1-3.

[53] Matsuda T, Kotanigawa T, Kataoka I, Naka A. 54 × 42.7 Gbit/s L- and U-band WDM signal transmission experiments with in-line hybrid optical amplifiers. Electron Lett 2004 Mar 18; 40(6): 380-1.

[54] Gnauck AH, Charlet G, Tran P, *et al.* 25.6-Tb/s WDM Transmission of Polarization - Multiplexed RZ-DQPSK Signals. J Lightwave Technol 2008; 26(1): 79-84.

[55] Maeda H, Funatsu G, Naka A. Ultra-long-span 500 km 16 × 10 Gbit/s WDM unrepeatered transmission using RZ-DPSK format. Electron Lett 2005; 41(1): 34-5.

[56] Rasmussen C, Fjelde T, Bennike J, *et al.* DWDM 40G transmission over trans-pacific distance (10000 km) using CSRZ-DPSK, enhanced FEC, and all- Raman-amplified 100-km UltraWave fiber spans. J Lightwave Technol 2004; 22: 203-7.

[57] Fukai C, Nakajima K, Kurokawa K, *et al*. Applicability of silica core photonic crystal fiber for distributed Raman amplification transmission. Opt Fiber Technol 2008; 14(3): 196-202.

[58] Zhang T, Zhang XP, Zhang GD. Distributed fiber Raman amplifiers with incoherent pumping. IEEE Photonics Technol Lett 2005; 17(6): 1175-7.

[59] Andre PS, Pinto AN, Teixeira ALJ, *et al*. Raman Amplification using Incoherent Pump Sources. In: International Conference Transparent Optical Networks; 2007. pp. 136-9.

[60] Kaewplung P, Kikuchi K. Simultaneous cancellation of fiber loss, dispersion, and Kerr effect in ultralong-haul optical fiber, transmission by midway optical phase conjugation incorporated with distributed Raman amplification. J Lightwave Technol 2007; 25(10): 3035-50.

[61] Bakhshi B, Papernyi SB, Manna M, *et al*. 320 Gb/s (32/spl times/12.3 Gb/s) 410 km repeaterless WDM system ready for field deployment. In: European Conference in Optical Communication 2005. pp. 73-4.

[62] Masuda H, Tomizawa M, Miyamoto Y. High-performance distributed Raman amplification systems: practical aspects and field trial results. In: Optical Fiber Communication Conference 2005; p. 3.

[63] Schneiders M, Vorbeck S, Leppla R, *et al*. Field transmission of 8/spl times/170 Gbit/s over high loss SSMF link using third order distributed Raman amplification. In: Optical Fiber Communication Conference; 2005. p. 3.

[64] Tashiro Y, Koyanagi S, Aiso K, Namiki S. 1.5-W erbium-doped fiber amplifier pumped by the wavelength division-multiplexed 1480 nm laser diodes with fiber Bragg grating. In: Optical Amplifiers and Their Applications; 1998. pp. WC2.

[65] Xiangjun X, Chongxiu Y, Jianhua R, *et al.* Experimental investigation of the performance of co- and counter-pumped Raman fiber amplifiers. Micro Optical Technol Lett 2003 May 5; 37(3): 190-4.

[66] Stentz AJ, Nielsen T, Grubb SG, Strasser TA, Pedrazzani JR. Raman ring amplifier at 1.3 μm with analog-grade performance and an output power of 23 dBm. In: Optical Fiber Communication Conference 1996. pp. PD16.

[67] Hansen PB, Jacobovitz-Veselka G, Gruner-Nielsen L, Stentz AJ. Raman amplification for loss compensation in dispersion compensating fibre modules. Electron Lett 1998; 34(11): 1136-7.

[68] Emori Y, Akasaka Y, Namiki S. Broadband lossless DCF using Raman amplification pumped by multichannel WDM laser diodes. Electron Lett, 1998; 34(22): 2145-6.

[69] Gruner-Nielsen L, Yujun Q, Palsdottir B, Gaarde PB, Dyrbol S, Veng T. Module for simultaneous C+L-band dispersion compensation and Raman amplification. In: Optical Fiber Communication conference 2002. pp. 65-6.

[70] Ishikawa E, Nishihara M, Sato Y, Ohshima C, Sugaya Y, Kumasako J. Novel 1500 nm band EDFA with discrete Raman amplifier. In: European Conference on Optical Communication 2001. pp. 48-9.

[71] Miyamoto T, Tsuzaki T, Okuno T, *et al.* Raman amplification over 100 nm-bandwidth with dispersion and dispersion slope compensation for conventional single mode fiber. In: Optical Fiber Communication Conference; 2002. pp. 66-8.

[72] Han YG, Lee JH, Kim SH, Lee SB. Tunable multi-wavelength Raman fibre laser based on fibre Bragg grating cavity with PMF Lyot-Sagnac filter. Electron Lett 2004; 40(23): 1475-6.

[73] Bellemare A, Karasek M, Rochette M, LaRochelle S, Tetu M. Room temperature multifrequency erbium-doped fiber lasers anchored on the ITU frequency grid. J Lightwave Technol 2000; 18(6): 825-31.

[74] Wang ZY, Cui YP, Yun BF, Lu CG. Multiwavelength generation in a Raman fiber laser with sampled Bragg grating. IEEE Photon Technol Lett 2005; 17(10): 2044-6.

[75] Han YG, Kim CS, Kang JU, Paek UC, Chung Y. Multiwavelength Raman fiber-ring laser based on tunable cascaded long-period fiber gratings. IEEE Photon Techn Lett 2003; 15(3): 383-5.

[76] Dong XY, Shum P, Ngo NQ, Chan CC. Multiwavelength Raman fiber laser with a continuously-tunable spacing. Opt Express 2006; 14(8): 3288-93.

[77] de Matos CJS, Chestnut DA, Reeves-Hall PC, Koch F, Taylor JR. Multi-wavelength, continuous wave fibre Raman ring laser operating at 1.55 um. Electron Lett 2001; 37(13): 825-6.

[78] Kim NS, Zou X, Lewis K. CW depolarized multiwavelength Raman fiber ring laser with over 58 channels and 50 GHz channel spacing. In: Optical Fiber Communication Conference 2002. pp. 640- 2.

[79] Kim CS, Sova RM, Kang JU. Tunable multi-wavelength all-fiber Raman source using fiber Sagnac loop filter. Opt Commun 2003 Apr 1; 218: 291-5.

[80] Chen LR. Tunable multiwavelength fiber ring lasers using a programmable high-birefringence fiber loop mirror. IEEE Photon Technol Lett 2004 Feb; 16(2): 410-2.

[81] Han YG, Tran TVA, Kim SH, Lee SB. Development of a multiwavelength Raman fiber laser based on phase-shifted fiber Bragg gratings for long-distance remote-sensing applications. Opt Lett 2005 May 15; 30(10): 1114-6.

[82] Han YG, Tran TVA, Kim SH, Lee SB. Multiwavelength Raman-fiber-laser-based long-distance remote sensor for simultaneous measurement of strain and temperature. Opt Lett 2005 Jun 1; 30(11): 1282-4.

[83] Han YG, Moon DS, Chung YJ, Lee SB. Flexibly tunable multiwavelength Raman fiber laser based on symmetrical bending method. Opt Express 2005 Aug 22; 13(17): 6330-5.

[84] Han YG, Lee SB, Moon DS, Chung Y. Investigation of a multiwavelength Raman fiber laser based on few-mode fiber Bragg gratings. Opt Lett 2005 Sep 1; 30(17): 2200-2.

[85] Wang ZY, Cui YP, Yun BF, Lu CG. Multiwavelength generation in a Raman fiber laser with sampled Bragg grating. IEEE Photonics Technol Lett 2005 Oct; 17(10): 2044-6.

[86] Ning G, Shum P, Zhou JO, Xia L. Multiwavelength Raman fiber laser inserting a sampled chirped fiber Bragg grating. Micro Opt Techol Lett 2007 Sep; 49(9): 2242-5.

[87] Kee HH, Lees GP, Newson TP. 1.65 um Raman-based distributed temperature sensor. Electron Lett 1999 Oct 14; 35(21): 1869-71.

[88] Farahani MA, Gogolla T. Spontaneous Raman scattering in optical fibers with modulated probe light for distributed temperature Raman remote sensing. J Lightwave Technol 1999 Aug; 17(8): 1379-91.

[89] Diaz S, Lopez-Amo M. Comparison of wavelength-division-multiplexed distributed fiber Raman amplifier networks for sensors. Opt Express 2006 Feb 20; 14(4): 1401-7.

[90] Lee JH, Kim J, Han YG, Kim SH, Lee SB. Investigation of Raman fiber laser temperature probe based on fiber Bragg gratings for long-distance remote sensing applications. Opt Express 2004 Apr 19; 12(8): 1747-52.

[91] Jung J, Park N, Lee B. Simultaneous measurement of strain and temperature by use of a single fiber Bragg grating written in an erbium : ytterbium-doped fiber. Appl Opt 2000 Mar 1; 39(7): 1118-20.

[92] Peng PC, Tseng HY, Chi S. Long-distance FBG sensor system using a linear-cavity fiber Raman laser scheme. IEEE Photonics Technol Lett 2004 Feb; 16(2): 575-7.

[93] Tran TVA, Han YG, Kim SH, Lee SB. Long-distance simultaneous measurement of strain and temperature based on a fiber Raman laser with a single fiber Bragg grating embedded on a quartz plate. Opt Lett 2005 Jul 1; 30(13): 1632-4.

[94] Tran TVA, Han YG, Lee HYJ, Kim SH, Lee SB. Performance enhancement of long-distance simultaneouis measurement of strain and temperature based on a fiber Raman laser with an etched FBG. IEEE Photon Technol Lett 2005 Sep; 17(9): 1920-2.

[95] Lee JH, Chang YM, Han YG, Chung H, Kim SH, Lee SB. Raman amplifier-based long-distance remote, strain and temperature sensing system using an erbium-doped fiber and a fiber Bragg grating. Opt Express2004 Jul 26; 12(15): 3515-20.

[96] Cho YT, Alahbabi MN, Brambilla G, Newson TP. Distributed Raman amplification combined with a remotely pumped EDFA utilized to enhance the performance of spontaneous Brillouin-based distributed temperature sensors. IEEE Photon Technol Lett 2005 Jun; 17(6): 1256-8.

[97] Gong YD, Michael OLC, Hao JZ, Paulose V. Extension of sensing distance in a ROTDR with an optimized fiber. Opt Commun 2007 Dec 1; 280(1): 91-4.

[98] Chakraborty AL, Sharma RK, Saxena MK, Kher S. Compensation for temperature dependence of stokes signal and dynamic self-calibration of a Raman distributed temperature sensor. Opt Commun 2007 Jun 15; 274(2): 396-402.

[99] Yusoff Z, Lee JH, Belardi W, Monro TM, Teh PC, Richardson DJ. Raman effects in a highly nonlinear holey fiber: amplification and modulation. Opt Lett 2002 Mar 15; 27(6): 424-6.

[100] Fuochi M, Poli E, Selleri S, Cucinotta A, Vincetti L. Study of Raman amplification properties in triangular photonic crystal fibers. J Lightwave Technol 2003 Oct; 21(10): 2247-54.

[101] Bottacini M, Poli F, Cucinotta A, Selleri S. Modeling of photonic crystal fiber Raman amplifiers. J Lightwave Technol 2004; 22(7): 1707-13.

[102] Yiou S, Delaye P, Rouvie A, *et al.* Stimulated Raman scattering in an ethanol core microstructured optical fiber. Opt Express 2005; 13(12): 4786-91.

[103] Tsang HK, Liu Y. Nonlinear optical properties of silicon waveguides. Semicond Sci Technol 2008; 23(6): 1-9.

[104] Claps R, Dimitropoulos D, Jalali B. Stimulated Raman scattering in silicon waveguides. Electron Lett 2002; 38(22): 1352-4.

[105] Rong HS, Liu AS, Jones R, *et al.* An all-silicon Raman laser. Nature 2005 Jan 20; 433(7023): 292-4.

[106] Liu AS, Rong HS, Jones R, Cohen O, Hak D, Paniccia M. Optical amplification and lasing by stimulated Raman scattering in silicon waveguides. J Lightwave Technol 2006; 24(3): 1440-55.

[107] Krause M, Renner H, Brinkmeyer E. Efficient Raman amplification in cladding-pumped silicon waveguides. In: 3rd IEEE International Conference on Group IV Photonics 2006. pp. 61-3.

[108] Krause M, Renner H, Fathpour S, Jalali B, Brinkmeyer E. Gain enhancement in cladding-pumped silicon Raman amplifiers. IEEE J Quantum Electron 2008; 44: 692-704.

Received: October 6, 2008 Revised: December 23, 2008 Accepted: December 23, 2008